10 PET for Therapy Response Assessment in Glioblastoma

JULIE BOLCAEN[1] • MARJAN ACOU[2] • BENEDICTE DESCAMPS[3] • KEN KERSEMANS[1] • KAREL DEBLAERE[2] • CHRISTIAN VANHOVE[3] • INGEBORG GOETHALS[1]

[1]Department of Nuclear Medicine, Ghent University Hospital, Ghent, Belgium; [2]Department of Radiology and Medical Imaging, Ghent University Hospital, Ghent, Belgium; [3]IBiTech-MEDISIP, Department of Electronics and Information Systems, Ghent University, Ghent, Belgium

Author of correspondence: Julie Bolcaen, Department of Nuclear Medicine, Ghent University Hospital, Ghent, Belgium. E-mail: Julie.Bolcaen@ugent.be

Doi: http://dx.doi.org/10.15586/codon.glioblastoma.2017.ch10

Abstract: Glioblastoma (GB) is the most malignant and the most common type of glioma in adults, accounting for 60–70% of all malignant gliomas. Despite the current therapy, the clinical course of GB is usually rapid, with a mean survival time of approximately 1 year. For therapy response assessment in GB, magnetic resonance imaging (MRI) is the method of choice. In 2010, the Response Assessment in Neuro-Oncology (RANO) was introduced, including the tumor size (in 2D) as measured on T2-weighted and Fluid Attenuated Inversion Recovery (FLAIR)-weighted images, in addition to the contrast-enhancing tumor part. Although the RANO criteria addressed some of the limitations of the previous MacDonald criteria for therapy evaluation in high-grade glioma, treatment-related side effects hamper correct response assessment. To address the above-mentioned drawbacks in the follow-up of GB, incorporating changes in tumor biology measured by advanced MRI and positron emission tomography (PET) imaging, which may precede anatomical changes of the tumor volume, is promising. Imaging biomarkers capable of predicting response at an early time point after treatment initiation are the premise of personalized treatment enabling change or

In: *Glioblastoma*. Steven De Vleeschouwer (Editor), Codon Publications, Brisbane, Australia
ISBN: 978-0-9944381-2-6; Doi: http://dx.doi.org/10.15586/codon.glioblastoma.2017

discontinuation of therapy to prevent ineffective treatment or adverse events of treatment. In this chapter, an overview of applicable PET tracers for the therapy response assessment in GB and the determination of tumor recurrence versus treatment-related effects is given.

Key words: Glioblastoma; MRI; PET; Radiation necrosis; Therapy response

Introduction

Gliomas are the most common primary brain tumors with a peak incidence in the fifth and sixth decade of life (1, 2). The highest grade of gliomas (WHO grade IV) are called glioblastoma (GB). GBs account for more than half of all glial tumors, are a highly invasive solid tumor type, and are most often found in cerebral hemispheres, particularly in frontal, parietal, and temporal lobes, although they can be situated in any lobe. They can arise *de novo* (primary GB) or after progression of a low-grade glioma (secondary GB) (2–4). Usually, GBs are poorly delineated, heterogeneous tumors with necrosis, hemorrhage, and increased vascularity. Central necrosis is the hallmark of GBs and may occupy as much as 80% of total tumor mass (2). GB cell infiltration into the surrounding brain parenchyma renders a complete surgical resection mostly impossible without producing significant neurological injury. Residual glioma cells at the tumor margins frequently lead to tumor recurrence (3). In patients with suspected brain tumor, after medical history taking and clinical examination, the most important diagnostic procedure is magnetic resonance imaging (MRI) of the brain with a contrast-enhancing agent. However, the diagnosis should be confirmed via a stereotactic biopsy or, when appropriate, via resection. Functional and molecular imaging has gained a lot of attention in the last decade. Before confirmation of the diagnosis via tissue analysis, MR spectroscopy (MRS), perfusion weighted MRI (PWI), and positron emission tomography (PET) imaging can be helpful. After the diagnosis has been confirmed pathologically, these imaging modalities can be even more valuable. In particular, they may be useful for planning of radiation therapy (RT) and even more established in clinical practice for the monitoring during therapy, post-treatment surveillance, and prognostication (5, 6).

Treatment of Glioblastoma

Surgical resection remains one of the most effective treatments for cerebral gliomas (7, 8). It has been shown that patients who had a gross total resection also have a better response to subsequent adjuvant treatments than those who had only a partial resection or biopsy (7). However, in about half of the patients, (total) resection is not possible (9). The current standard of care for patients with GB has slowly evolved over the course of several decades. In the early 1960s, systemic corticosteroids were shown to have a beneficial impact on patients' quality of life by reducing peritumoral edema. Shortly thereafter, whole brain radiation therapy (WBRT) became recognized as an effective adjuvant therapy.

However, the dose was limited by potential toxicity to the surrounding normal brain (3). New developments in RT enabled to shape the radiation dose conform to the tumor target, limiting the dose to normal tissues, resulting in so-called conformal RT. Intensity-modulated radiation therapy (IMRT) allows even greater control over the shape of the dose distribution using variable intensities of the radiation beam (10, 11). In an effort to complement the beneficial effects of corticosteroids and RT, systemic chemotherapeutic agents were also studied (3). In 2005, Stupp et al. established the superiority of surgery and combined chemoradiation therapy with temozolomide (TMZ) over surgery and RT alone. As a result, for newly diagnosed GB patients with a good performance status, the standard of care now includes maximal surgical resection followed by combined external beam RT (60 Gy in 30 fractions) and TMZ, followed by maintenance TMZ (12–14). TMZ is an oral deoxyribonucleic acid (DNA) alkylating agent with good blood brain barrier (BBB) penetration. It is usually well tolerated with thrombocytopenia as its main and dose-limiting toxicity. In contrast to TMZ, nitrosoureas such as lomustine (CCNU), carmustine (BCNU), nimustine (ACNU), or fotemustine can induce prolonged leukopenia and thrombocytopenia, requiring dose reductions for the subsequent cycles, or a change of regimen. Nitrosoureas are now second-choice agents relative to TMZ for glioma treatment. In high-risk, low-grade gliomas, RT followed by procarbazine, CCNU, and vincristine (PCV) constitutes a new standard of care due to prolonged survival reported in the RTOG 9802 trial (15). The most recent development with respect to novel therapies for GB involves the use of angiogenesis inhibitors, such as bevacizumab, which improve the quality of life of patients due to their capacity to reduce vessel leakiness, resulting in diminished intracranial edema (16). Despite the current therapy for GB, the clinical course of GB tumors is usually rapid, with a mean survival time between 6 and 12 months (2).

THERAPY RESPONSE ASSESSMENT OF GLIOBLASTOMA

Several prognostic factors have been identified in patients with GB, such as age, Karnofsky performance status, neurological status, WHO tumor grade, tumor location, extent of surgery, genetic and molecular biomarker status, and concomitant TMZ (17, 18). For therapy response assessment in GB, MRI is the method of choice. Until 2010, mainly MacDonald criteria were used for assessing response to therapy in high-grade glioma (HGG). Although the MacDonald criteria were developed primarily for computed tomography (CT) scans, they have been extrapolated to MRI. The criteria are based on two-dimensional (2D) tumor measurements on CT or MRI, in addition to a clinical assessment and corticosteroid use and dose (19). In the MacDonald criteria, a significant increase (≥25%) in the contrast-enhancing lesion is used as a reliable marker for tumor progression. However, contrast enhancement after the administration of gadolinium is nonspecific and primarily reflects the passage of contrast material across a disrupted BBB. Furthermore, in 20–30% of patients, pathological contrast enhancement on MRI subsiding without any change in therapy is shown on the first post-irradiation MRI. This phenomenon, known as *pseudoprogression*, likely results from a combination of transiently increased permeability of the tumor vasculature from irradiation, treatment-induced necrosis, and post-operative infarcts, and should always

be considered in the first 3 months after concurrent chemoradiation for gliomas (19–21). In addition, it is worth mentioning that pseudoprogression may be reinforced by chemotherapy with TMZ (9, 19, 22). This treatment-related effect complicates the determination of tumor progression immediately after the completion of RT and may result in premature discontinuation of effective adjuvant therapy (19, 22). Furthermore, since the introduction of antiangiogenic agents, another phenomenon known as "*pseudoresponse*" occurred. These agents can produce a marked decrease in contrast enhancement as early as 1–2 days after initiation of therapy, which may be partly a result of normalization of abnormally permeable tumor vessels and not a true anti-glioma effect as a nonenhancing tumor may continue to grow (19, 20). This normalization of BBB disruption is often combined with a regression of perifocal edema followed by an improvement of neurological symptoms and consequently a reduction of corticosteroid use (22). In an attempt to more accurately assess treatment response, new criteria for Response Assessment in Neuro-Oncology (RANO) were introduced in 2010, including the tumor size (in 2D) as measured on T2-weighted and Fluid Attenuated Inversion Recovery (FLAIR)-weighted images, in addition to the contrast-enhancing tumor part. Although the RANO criteria addressed some of the limitations of the MacDonald criteria for evaluation of therapy in HGG, the abovementioned treatment-related side effects hamper correct response assessment. The proposed new response criteria suggest that within the first 3 months after completion of RT, progression can only be determined if the majority of the new enhancement is outside of the radiation field or if there is pathologic confirmation of progressive disease. This means that response assessment shortly after the end of RT is not accepted (22). Furthermore, increased enhancement and FLAIR/T2 hyperintense signal abnormalities can also occur due to treatment-related inflammation, postsurgical changes, subacute irradiation effects, and radiation necrosis (RN) (19). As such, tumor recurrence cannot be accurately distinguished from treatment effects on CT or conventional MRI (9).

DIFFERENTIATION BETWEEN TREATMENT-RELATED EFFECTS AND GLIOBLASTOMA RECURRENCE

Early and late therapy-related effects on brain tissues are an unwanted but unavoidable consequences of RT (7). The incidence is increasing with more frequent use of stereotactic radiosurgery and combined modality therapy for brain tumors. These therapy-related effects on the brain, such as radiation injury, also add to the complexity of imaging response and recurrence patterns, which is particularly important in patients with HGG in whom recurrence is commonly seen (20, 21). Radiation injury is known to potentially target glial cells and vascular endothelial cells and has been divided into acute, early-delayed, and late-delayed reactions (20, 23). Acute RN (during RT to 3 months after completion of RT) is a consequence of injury to the vasculature, more specifically radiation-induced endothelial cell apoptosis, leading to capillary leakiness and edema. Up to 12 weeks following RT, early-delayed injury can occur due to a delay in myelin synthesis (injury to oligodendrocytes). However, pseudoprogression must be considered. Late vascular changes include vessel wall thickening, with resulting occlusive vasculopathy, perivascular parenchymal coagulative necrosis,

and inflammation. Late delayed reactions are reported to occur in 3–24% of patients from 3 months to 13 years after the completion of RT (23–26). The risk increases with increasing radiation dose, fraction size, irradiated volume, and the (concomitant) administration of chemotherapy (24). The pattern of radiation injury may vary from diffuse periventricular white matter lesions to focal or multifocal lesions and may occur even distant from the original site of treatment (27). Differentiation between RN and recurrent brain tumor presents a diagnostic dilemma as both entities frequently develop at the resection site and often have a similar appearance on conventional MRI (20, 21). Both types of lesions can have similar clinical presentations, such as seizures, focal neurologic deficits, and increased intracranial pressure (25). Obviously, a correct diagnosis is important for further patient management. RN may require the administration of steroids, whereas tumor recurrence necessitates second-line treatment (20, 28). A definite diagnosis requires a biopsy. Unfortunately, a biopsy is subject to sampling error, is invasive, and can lead to potential complications such as brain hemorrhage (21).

To address the abovementioned drawbacks in the follow-up of GB, incorporating changes in tumor biology measured by advanced MRI and PET imaging, which may precede anatomical changes of the tumor volume, is promising (9, 29, 30). Imaging biomarkers able to predict response at an early time point after treatment initiation are the premise of personalized treatment enabling change or discontinuation of therapy to prevent ineffective treatment or adverse events of treatment. Moreover, identification of treatment failure may help reduce costs. This is highly relevant because the expense of newer systemic treatment options (e.g., bevacizumab) is considerably higher than conventional alkylating chemotherapy (e.g., lomustine) (31). Currently, MRI techniques that interrogate the vascular density and permeability of tumor vasculature, such as dynamic contrast-enhanced MRI (DCE-MRI), diffusion-weighted MRI (DWI), perfusion-weighted MRI (PWI), and metabolite concentrations using MRS, are being evaluated as imaging biomarkers of tumor response in treatment trials (9). Using DWI, higher apparent diffusion coefficients (ADCs) were found in RN compared to tumor recurrence due to an increase in water in the interstitial spaces resulting from cell necrosis (32). Choline/creatine and choline/*N*-acetylaspartate ratios as measured by MRS may also add valuable information in differentiating recurrent tumor from RN, and even a higher diagnostic accuracy was achieved when combining DWI with MRS (32, 33). PWI, such as dynamic susceptibility contrast-enhanced MRI (DSC-MRI), was found to distinguish tumor recurrence from RN by using cerebral blood volume (CBV) maps (9, 34–36). Furthermore, the use of the amide proton transfer MRI signal of endogenous cellular proteins and peptides as an imaging biomarker has been shown to be able to differentiate viable glioma from RN in rats (37). Although advanced MRI techniques may yield promising results, a major disadvantage is the current lack of standardization and validation, which hampers the translation into the clinic. In the remainder of this chapter, the focus is on the use of PET for therapy response assessment in GB. In the future, incorporation of these advanced imaging techniques into the RANO criteria is necessary, but it needs standardization and requires rigorous clinical validation before they can be recommended and incorporated into response criteria (19). Currently, the decision tree given in Figure 1 can be proposed for the follow-up of HGG (38).

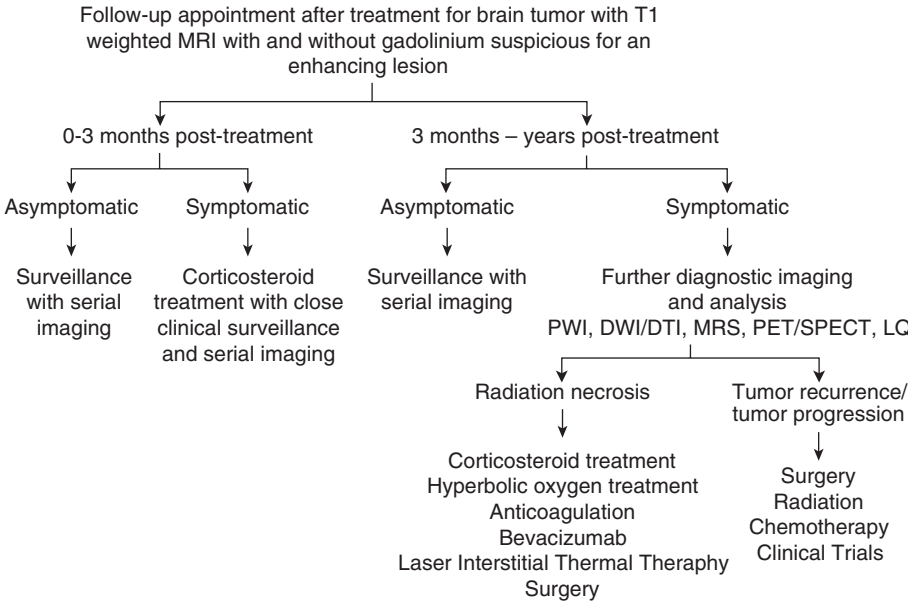

Figure 1 Decision tree for post-treatment follow-up in high-grade gliomas. (Adapted from Ref. (38).)

PET for Therapy Response Assessment in GB

In the past decades, a variety of molecular targets have been addressed by specific PET tracers in neuro-oncology and could be used for therapy response evaluation in HGG, see Figure 2 (39–44).

^{18}F-FLUORODEOXYGLUCOSE (^{18}F-FDG) PET

^{18}F-Fluorodeoxyglucose (^{18}F-FDG) is the most common clinically utilized PET tracer due to its high potential to detect tumors in the body based on increased energy demand of malignant tumors. ^{18}F-FDG PET measures cellular glucose metabolism as a function of the enzyme hexokinase (40, 41, 45). ^{18}F-FDG-6-PO_4 accumulates in cells over time, leading to signal amplification and making this imaging agent a suitable indicator of hexokinase-II activity as well as a cell's need for glucose (45). In the brain, ^{18}F-FDG exhibits high uptake in normal gray matter, reflecting the metabolic demands of neurons and glia. This high uptake in normal brain parenchyma often makes the localization and the delineation of brain tumors difficult and only co-registration of ^{18}F-FDG PET with MRI allows the rating of glucose metabolism in specific areas of a tumor, see Figure 2A (40, 41). Several studies investigating the potential of ^{18}F-FDG in discriminating tumor recurrence and RN have been performed. However, equivocal results with sensitivities and specificities ranging from 40 to 100% were published (21, 28, 34, 46–48). Besides the high and variable uptake by the normal cortex, radiation

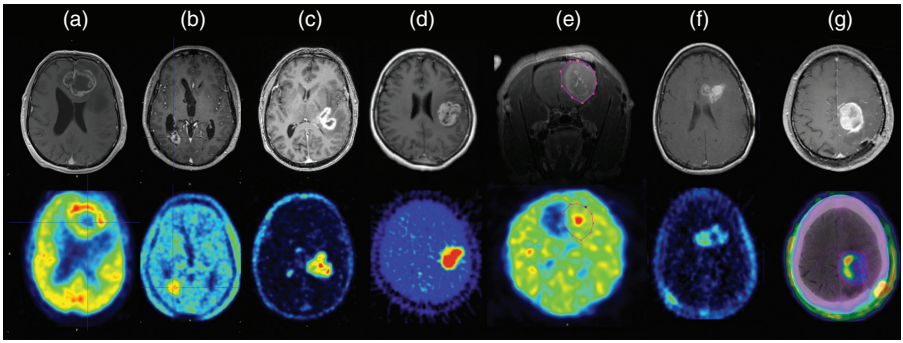

Figure 2 Contrast-enhanced MRI (top row) and multiple PET tracers (bottom row) in glioblastoma. (a) ^{18}F-Fluorodeoxyglucose (^{18}F-FDG), (b) ^{18}F-fluoroethyltyrosine (^{18}F-FET), (c) ^{18}F-Fluoromethylcholine (^{18}F-FCho), (d) ^{18}F-fluoromisonidazole (^{18}F-FMISO) (43) PET in human GB, (e) ^{18}F-fluoroazomycin arabinoside (^{18}F-FAZA) PET of the rat F98 model, (f) ^{18}F-fluorothymidine (^{18}F-FLT) (9) PET, and (g) ^{18}F-AIF-NOTA-PRGD2 (^{18}F-RGD) PET/CT in human GB. (Adapted from Ref. (44).)

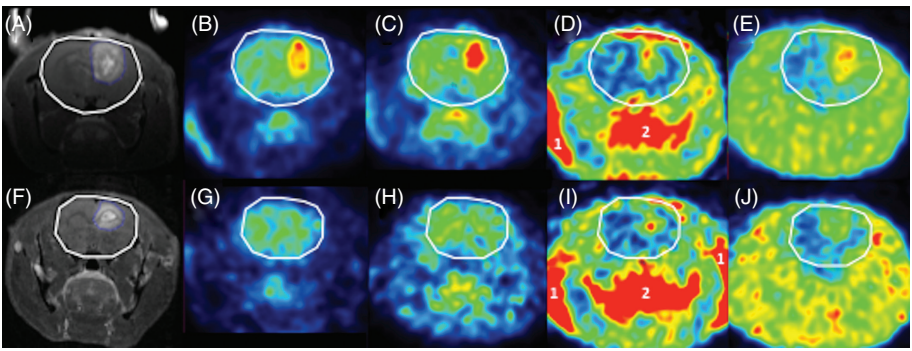

Figure 3 Contrast-enhanced MRI (A and F) and PET of glioblastoma (top row) and radiation necrosis (bottom row). For clarity, the rat brain is contoured in white. ^{18}F-FDG PET 40-60 min post-injection (B,G) and 240 min post-injection (C,H), ^{18}F-FCho PET 10-20 min post-injection (D,I), ^{18}F-FET PET 35-55 min post-injection (E,J) (49).

injury can activate repair mechanisms or lead to inflammation, which can lead to false-positive results (20).

Our research group compared the uptake of ^{18}F-FDG, ^{18}F-fluoromethylcholine (^{18}F-FCho), and ^{18}F-fluoroethyltyrosine (^{18}F-FET) in GB and RN in rats, see Figure 3 (49, 50). We found significantly higher values for the maximum and mean standard uptake value (SUV_{max} and SUV_{mean}) and the maximum and mean lesion to normal tissue ratio (LNR_{max} and LNR_{mean}) on ^{18}F-FDG PET in GB compared to RN. Uptake of ^{18}F-FDG in GB was high, which means that the uptake was higher than that in the cortex. The latter was not shown in RN (51, 52). In the literature, ^{18}F-FDG PET has been found to be of only moderate additional value to MRI for differentiation between glioma recurrence and RN, especially due to low specificity (6, 21, 28, 30, 48, 53, 54). A potentially useful approach for

^{18}F-FDG PET is dual-phase imaging. It was shown previously that delayed ^{18}F-FDG imaging 3–8 h after injection improves the distinction between tumor and normal gray matter because the outflow of glucose was hypothesized to be higher from normal brain tissue than from the tumor. This was confirmed using kinetic modeling (KM) showing that the dephosphorylation rate of FDG-6 phosphate values were not significantly different between tumor and normal brain tissue at early imaging times but was lower in tumor than in normal brain tissue at delayed imaging times (55–58). Applying conventional and delayed ^{18}F-FDG PET, Horky et al. found that early and late SUVs of the lesion alone did not differentiate between tumor and necrosis. However, the change of LNR_{max} between early and late ^{18}F-FDG images was 95% sensitive, 100% specific, and 96% accurate (58). In our study, we found that differences in LNR_{mean} and LNR_{max} between GB and RN were higher on the delayed PET images compared to the conventional ^{18}F-FDG PET. A plausible explanation is that, like normal brain tissue, necrotic tissue shows increased ^{18}F-FDG excretion at delayed times when compared with tumor (56). Consequently, the LNR increases over time for tumor but remained stable or even decreased for RN (58).

AMINO-ACID PET

Radiolabeled amino acids are the most commonly used PET tracers for imaging brain tumors. An advantage over ^{18}F-FDG is the relatively low uptake of amino acids by normal brain tissue. Therefore, cerebral gliomas can be distinguished from the surrounding normal tissue with higher contrast, see Figure 2B (40, 41). Labeled amino acid tracers developed so far for PET imaging are divided into two categories: tracers actively incorporated into the proteins, such as ^{11}C-Methionine (^{11}C-MET), potentially allowing investigating protein synthesis, and tracers not integrated into proteins, such as ^{18}F-fluoroethyltyrosine (^{18}F-FET) and 3,4-dihydroxy-6-^{18}F-fluoro-l-phenylalanine (^{18}F-FDOPA), which are valuable tools to evaluate amino acid transport (59). The increased uptake of ^{18}F-FET and ^{18}F-FDOPA by cerebral glioma tissue appears to be caused mainly by increased transport via sodium-independent amino acid transport system L for large neutral amino acids (LATs) and Na^+-dependent general amino acid transporters $B^{0,+}$ and B^0, with a disruption of the BBB not being a prerequisite for intratumoral accumulation (20, 60–62). Most PET studies of cerebral gliomas have been performed with ^{11}C-MET, although the short half-life of ^{11}C (20 min) limits the use of this tracer to the few centers that are equipped with an on-site cyclotron facility. Results with ^{18}F-FET PET are similar to those with ^{11}C-MET (63), and due to its longer half-life (109 min) and lack of (or minimal) uptake in macrophages and inflammatory cells, ^{18}F-FET PET is preferred for clinical use (56, 59, 61, 64–67). The diagnostic potential of ^{18}F-FET PET in brain tumors is well documented, for example, a superior delineation of human gliomas by ^{18}F-FET PET compared with MRI and a high specificity for the detection of gliomas and biopsy site planning (31, 64, 68). Among WHO grades III and IV gliomas, the vast majority (>95%) shows increased ^{18}F-FET uptake. However, a lack of ^{18}F-FET uptake does not exclude a glioma, as approximately one-third of WHO grade II gliomas and most dysembryoplastic neuroepithelial tumors (WHO grade I) are ^{18}F-FET negative (6). Several studies have also indicated that

time–activity curves of ^{18}F-FET uptake contain biological information beyond that of static images, and these data may be helpful for glioma grading (31). In HGGs, uptake patterns of ^{18}F-FDOPA are not significantly different from ^{18}F-FET, but both SUV_{mean} and LNRs were 10–15% higher for ^{18}F-FET than ^{18}F-FDOPA (69).

Current amino acid PET data suggest that deactivation of amino acid transport and/or decrease of the metabolically active tumor volume is a sign of treatment response associated with long-term outcome (6, 70–73). Treatment response and outcome in bevacizumab therapy has been suggested to be better assessed by ^{18}F-FET and ^{18}F-FDOPA, compared to MRI (6, 74–77). Also, reliable monitoring of TMZ and nitrosourea-based chemotherapy effects has been demonstrated in patients with recurrent HGG (9, 31, 64, 66, 70, 71). In a study by Rachinger et al., ^{18}F-FET PET was able to distinguish tumor progression from stable disease with 93% specificity and 100% sensitivity, while the specificity of conventional MRI alone was 50% (78). ^{18}F-FET PET responders, based on a decrease of more than 10% of LNR after completion of therapy, also showed a significant longer overall survival than nonresponders (60). The biological tumor volume on ^{18}F-FET PET prior to chemoradiotherapy and as early as 7–10 days after the completion of treatment in GB was also found to be highly prognostic. Remarkably, the time-to-peak and the shape of the ^{18}F-FET time–activity curve, derived from dynamic PET acquisitions, were shown to have value in therapy response assessment (6, 60, 70, 79, 80).

A promising role of amino acid PET for the distinction between tumor recurrence and benign post-therapeutic changes has also been suggested. The LNR of ^{11}C-MET PET revealed a sensitivity and specificity of 70–80% for the differentiation of brain metastasis recurrence from radiation-related effects (31). A higher diagnostic accuracy was shown by Grosu et al., with ^{11}C-MET able to differentiate tumor tissue from treatment-related changes with a sensitivity of 91% and a specificity of 100% (63). Using ^{18}F-FET PET, the detection of tumor recurrence/progression was even more accurate, with a sensitivity and specificity of 100% and 93%, respectively, compared with 93- and 50% for MRI alone (73, 78). Pöpperl et al. were able to distinguish recurrent tumor and RN with 100% accuracy, applying a threshold of 2.0 for LNR_{max}, and Galldiks et al. suggested that the combined evaluation of the LNR_{mean} of ^{18}F-FET uptake and the pattern of the time–activity curve can differentiate brain metastasis recurrence from RN with high accuracy (70, 73). The lower specificity of ^{11}C-MET may be explained by its higher affinity for macrophages compared with ^{18}F-FET as demonstrated in animal experiments (81, 82). In our study, ^{18}F-FET uptake in GB was more intense and more heterogeneous compared to RN, see Figure 3E. It was already mentioned that focal and high ^{18}F-FET uptake was suspicious for tumor recurrence, whereas low and homogeneous uptake around the resection cavity was considered benign due to post-treatment alterations of the BBB (73). Furthermore, amino acid PET was assumed to be superior to both ^{18}F-FCho PET and ^{18}F-FDG PET for diagnostic accuracy in distinguishing glioma recurrence from RN (6, 49, 50, 83). Using ^{18}F-FDOPA PET, a sensitivity and specificity of more than 80% to distinguish recurrent GB or recurrent brain metastasis and radiation-related effects was shown (25, 84). However, the lack of physiological ^{18}F-FET uptake in the basal ganglia when compared with ^{18}F-FDOPA PET makes ^{18}F-FET the most promising amino acid tracer for PET imaging in brain tumor patients (31).

However, it should be kept in mind that (moderately) increased ^{18}F-FET uptake can also be seen in acute inflammatory lesions such as active multiple sclerosis and brain abscesses (6).

^{18}F-FLUOROMETHYLCHOLINE (^{18}F-FCHO)

Positron-labeled choline analogues appear to be successful as oncological PET probes because a major hallmark of cancer cells is increased lipogenesis (85, 86). Phosphorylation by choline kinase (CK) constitutes an important step in the incorporation of choline into phospholipids, which is an essential component of all cell membranes. In cancer, there is often an increase in the cellular transport and phosphorylation of choline, as well as an increase in the expression of CK, increasing the uptake of radiolabeled choline (87–89). Choline can be labeled with either ^{11}C or ^{18}F. As a tracer, ^{11}C-Cho is biochemically indistinguishable from natural choline; however, the short half-life of ^{11}C has led to the development of ^{18}F-labeled derivatives, such as ^{18}F-Fluoromethylcholine (^{18}F-FCho) (90, 91). Previous *in vitro* studies have clearly documented that these fluorinated choline analogues are suitable substrates for the enzyme CK (90, 92), although the rate of their incorporation in phospholipids may be slower than that of endogenous choline (93). ^{18}F-labeled choline analogues have been investigated as oncological PET probes for the detection of (recurrent) local prostate cancer, but seem to have limited value for tumor and nodal staging. Rapidly proliferating GB cells have increased membrane/fatty acid requirements, which result in a higher ^{18}F-FCho uptake than in healthy brain tissue (86). Kwee et al. showed promising results for ^{18}F-FCho in brain tumor PET imaging with a differential uptake in HGG, brain metastases, and benign lesions (87). One of the assets of this tracer is the very low uptake in normal brain, increasing distinctively the contrast between GB and healthy brain, see Figure 2C. Changes in ^{18}F-FCho uptake may also precede post-treatment anatomical changes on conventional MRI (86). However, only a few studies investigated the potential of ^{18}F-FCho for therapy response assessment in gliomas. Li et al. reported that, for ^{11}C-Choline PET, an LNR≤1.4 might predict a longer overall survival in patients with suspected recurrent glioma after treatment (94). Parashar et al. suggested that there was a good correlation between a change in SUV_{max} of the tumor during RT and response (95). However, in the latter study, only one patient with a malignant glioma was included. Our research group recently investigated the potential of ^{18}F-FCho PET for early therapy response assessment in GB patients; see Figure 4 (96). Based on our results, ^{18}F-FCho SUV values pre-RT, during RT, and 1 month post-RT did not predict response. Physiological phenomena, such as therapy-induced perfusion changes due to alteration of BBB, cell repair mechanisms obscuring assessment of true cell death, and aspecific uptake of PET tracers due to infiltrating macrophages, may complicate response assessment. It should also be kept in mind that GBs are very heterogeneous tumors, containing clusters of tumor and normal cells, vascular structures, and necrotic tissues (29), which are not fully captured when using SUV_{max} or SUV_{mean} values. Based on our results, we also noted that in some nonresponders, absolute SUV values decreased during the course of the treatment while the metabolic tumor volume (MTV) increased, indicating that MTV is an important parameter. As such, we found that the ^{18}F-FCho PET-derived parameter, MTV x SUV_{mean}, allowed prediction of therapy

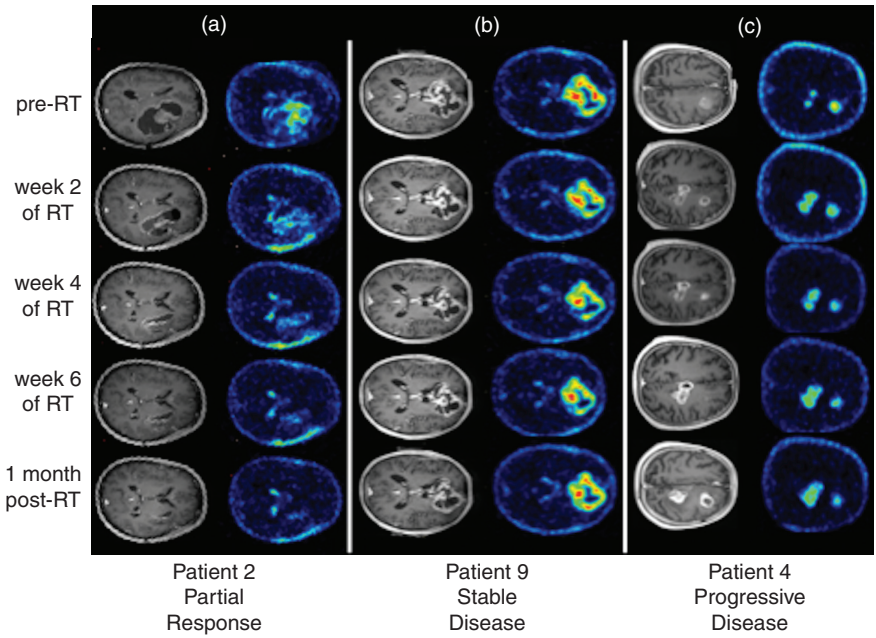

Figure 4 **^{18}F-Fluoromethylcholine (^{18}F-FCho) PET and contrast-enhanced T1-weighted MR images in 3 GB patients (a,b,c).** (a) A 47-year old female patient diagnosed with GB in the right frontal and temporal lobe. According to the RANO criteria the patient is categorized as a partial responder. A 60 % decrease in SUV_{max} and SUV_{mean} is observed from pre-RT to 1 month post-RT. (b) A 71-year old male patient diagnosed with a bifrontal GB. According to the RANO criteria, the patient was categorized as stable disease. From pre-RT to 1 month post-RT, SUV_{max} decreased 17 % while SUV_{mean} remained more or less stable. (c) A 66-year old male patient diagnosed with multifocal GB. A new lesion was visible on follow-up MRI, categorizing the patient as progressive disease. From pre-RT to 1 month post-RT SUV_{max} and SUV_{mean} decreased 52 % and 59 % respectively, while MTV increased with > 300 % (96).

response as early as 1 month after the completion of RT. Interestingly, the tumor volume derived from contrast-enhanced MRI was able to predict response earlier, that is, at week 6 during RT. However, due to the possibility of pseudoprogression, inclusion of PET in the RANO criteria might be helpful for early therapy response prediction in HGG.

Finally, ^{18}F-FCho PET was assumed to be promising in differentiating GB from RN (47, 52, 97). ^{18}F-FCho PET was studied in patients with solitary brain lesions and correctly identified patients with RN based on LNR (87). Tan et al. showed higher sensitivity and specificity for ^{11}C-Cho PET compared to MRI and ^{18}F-FDG, and Spaeth et al. noted a higher ^{18}F-FCho uptake in HGG compared to acute radiation injury (52, 97). Although promising results for the differentiation of RN and tumor recurrence in gliomas were reported, in our *in vivo* animal experiment, ^{18}F-FCho was not able to differentiate “pure” GB from “pure” RN; see Figure 3D (87, 97). Using KM and graphical analysis, we tried to interpret these results. However, we could not confirm an increased choline transporter-like protein-mediated transport, nor a higher expression of CK in GBs compared to RN.

The immediate metabolization of choline raises the question if ^{18}F-Fluorobetaine attributes to the detected choline signal, and the uptake in RN is influenced by leakage through the damaged BBB and inflammation (93, 98–101). As such, correlative imaging with MRI is of utmost importance (85). Also, it should be kept in mind that the metabolism of choline tracers in humans is slower than in rodents.

HYPOXIA-PET

Hypoxia is a pathological condition arising in living tissues when oxygen supply does not adequately cover the cellular metabolic demand. Detection of this phenomenon in tumors is of utmost clinical relevance because tumor aggressiveness, metastatic spread, failure to achieve local tumor control, increased rate of recurrence, and ultimate poor outcome are all associated with hypoxia (39, 102, 103). A number of hypoxia tracers are available for PET. The first introduced hypoxia tracer is called ^{18}F-fluoromisonidazole (^{18}F-FMISO). After passive diffusion through the membrane and in the presence of reduced pO_2, ^{18}F-FMISO undergoes progressive reduction by the nitroreductase enzyme (NTR). This process is reversible in the presence of sufficient O_2. Conversely, in hypoxic conditions, the reduced ^{18}F-FMISO is covalently bound to the intracellular proteins, resulting in tracer accumulation within the hypoxic cell (39, 40, 45, 88). To date, ^{18}F-FMISO has predominantly been used in a preclinical setting (79, 104). Concerning its use in therapy response assessment, the volume and intensity of hypoxia on ^{18}F-FMISO PET in GB before radiotherapy was strongly associated with poorer time to progression and survival (57). However, the slow uptake of ^{18}F-FMISO in target tissue and slow clearance of unbound ^{18}F-FMISO from nonhypoxic areas stimulated the development of ^{18}F-fluoroazomycin arabinoside (^{18}F-FAZA) with improved pharmacokinetics (39). A highly increased uptake of ^{18}F-FAZA was observed in all glioma types, with a LNR ranging between 2 and 16 due to low uptake in normal brain tissue (105). Also, in the F98 GB rat model, we observed a high LNR on ^{18}F-FAZA PET; see Figure 2D. Further prospective studies are however needed before incorporating hypoxia PET in glioma in the clinic. Another promising role for hypoxia PET lies in the era of PET-guided RT in GB.

^{18}F-FLUOROTHYMIDINE

DNA synthesis is required for cell growth and proliferation. Nucleotides of the four bases (cytosine, guanine, adenine, and thymidine) are required for DNA synthesis. Of these four nucleosides, thymidine is the only one incorporated exclusively into DNA, and not ribonucleic acid (RNA), providing a measure of DNA synthesis (106). ^{18}F-fluorothymidine (^{18}F-FLT) has been proposed to directly assess DNA synthesis to estimate tumor cell proliferation and has been proposed for therapy monitoring, based on the concept that change in DNA synthesis should be the most direct index of therapeutic effects on tumor proliferation (59). A direct correlation between ^{18}F-FLT uptake and Ki67 expression in tumor cells has been documented (56), leading to the use of this tracer in many tumor types as a surrogate for aggressiveness and an early marker of response (39, 56, 107–111). Obviously, tumor size is an important prognostic indicator, and tumor volume determined by ^{18}F-FLT was assumed to be a better predictor of overall survival than the intensity of uptake (112).

In preclinical GB models, early therapy response to chemotherapeutic and/or antiangiogenic therapy could be predicted via ^{18}F-FLT PET (113–115). This was confirmed in recurrent glioma patients treated with bevacizumab and irinotecan showing that ^{18}F-FLT is able to predict overall survival and would allow differentiation between recurrent glioma and RN (56, 116, 117). A high LNR of a GB tumor on ^{18}F-FLT PET is visible in Figure 2F (9). However, the sensitivity for the detection of HGG might be lower than required for clinical application, and dependence of ^{18}F-FLT uptake on BBB disruption raises the question of its specificity (59).

NOVEL PET TRACERS

Currently, novel promising glioma PET tracers are under investigation. The value of new amino acid PET tracers, such as α-^{11}C-methyl-tryptophan and ^{18}F-Fluciclovine as well as glutamine-based amino acid PET tracers has been evaluated with promising results in glioma patients in terms of tumor delineation, prognostication, and the differentiation of tumor recurrence from radiation injury (31, 118–122). Another interesting new PET target is the translocator protein (TSPO), a mitochondrial membrane protein highly expressed in activated microglia, macrophages, and neoplastic cells. Imaging with the TSPO ligand ^{11}C-(R)PK11195 demonstrates increased binding in HGG compared to low-grade gliomas and normal brain parenchyma (123, 124). More recently, the TSPO ligand ^{18}F-DPA-714 has been evaluated in glioma animal models, but results in human glioma patients are pending (31, 125, 126). A novel labeled integrin $\alpha_v\beta_3$-targeting ^{18}F-AIF-NOTA-PRGD2 (^{18}F-RGD) tracer showed positive results in assessing sensitivity to concurrent chemoradiotherapy in GB. An example is given in Figure 2G (44, 26). Another approach was published by Oborski et al., suggesting the ability to image therapy-induced tumor cellular apoptosis using ^{18}F-2-(5-fluoro-pentyl)-2-methyl-malonic acid (^{18}F-ML-10) for early therapy response assessment of a newly diagnosed GB patient (127).

Conclusion

The identification of new MRI and PET biomarkers and their inclusion in the RANO criteria may be helpful for early therapy response prediction in HGG. However, it is difficult to compare results of individual studies because of methodological differences and varying clinical endpoints (128). As such, standardization and validation are needed first.

Acknowledgment: The authors would like to thank Stichting Luka Hemelaere and Soroptimist International for supporting this work.

Conflict of interest: The authors declare no potential conflicts of interest with respect to research, authorship, and/or publication of this manuscript.

References

1. Omuro A, DeAngelis LM. Glioblastoma and other malignant gliomas. A clinical review. JAMA. 2013;310(17):1842–50. http://dx.doi.org/10.1001/jama.2013.280319
2. Drevelegas A, Karkavelas G. Imaging of brain tumors with histological correlations. Berlin: Springer; 2011. Chapter 6, High-grade gliomas; p. 157. http://dx.doi.org/10.1007/978-3-540-87650-2
3. Wadajkar AS, Dancy JG, Hersh DS, Anastasiadis P, Tran NL, Woodworth GF, et al. Tumor-targeted nanotherapeutics: Overcoming treatment barriers for glioblastoma. Wiley Interdiscip Rev Nanomed Nanobiotechnol. 2017;9(4):1–17. http://dx.doi.org/10.1002/wnan.1439
4. Huse JT, Holland EC. Targeting brain cancer: Advances in the molecular pathology of malignant glioma and medulloblastoma. Nat Rev Cancer. 2010;10(5):319–31. http://dx.doi.org/10.1038/nrc2818
5. Hattingen E, Pilatus U. Brain tumor Imaging. Berlin: Springer; 2016. Chapter, Brain tumor imaging; p. 1–11. http://dx.doi.org/10.1007/978-3-642-45040-2
6. Albert NL, Weller M, Suchorska B, Galldiks N, Soffietti R, Kim MM, et al. Response Assessment in Neuro-Oncology working group and European Association for Neuro-Oncology recommendations for the clinical use of PET imaging in gliomas. Neuro Oncol. 2016;18(9):1199–208. http://dx.doi.org/10.1093/neuonc/now058
7. Rees JH. Diagnosis and treatment in neuro-oncology: An oncological perspective. Br J Radiol. 2011;84:S82–9. http://dx.doi.org/10.1259/bjr/18061999
8. Watts C, Sanai N. Surgical approaches for the gliomas. Handbook Clin Neurol. 2016;134:51–69. http://dx.doi.org/10.1016/B978-0-12-802997-8.00004-9
9. Ahmed R, Oborski MJ, Hwang M, Lieberman FS, Mountz JM. Malignant gliomas: Current perspectives in diagnosis, treatment, and early response assessment using advanced quantitative imaging methods. Cancer Manag Res. 2014;6:149–70.
10. Khan FM. The physics of radiation therapy. 5th ed. Baltimore, MD: Wolters Kluwer Health—Lippincott Williams & Wilkins; 2010. Chapter 20, Intensity-modulated radiation therapy; p. 430.
11. Kirsch DG, Tarbell NJ. Conformal radiation therapy for childhood CNS tumors. Oncologist. 2004;9(4):442–50. http://dx.doi.org/10.1634/theoncologist.9-4-442
12. Stupp R, Dietrich PY, Ostermann Kraljevic S, Pica A, Maillard I, Maeder P, et al. Promising survival for patients with newly diagnosed glioblastoma multiforme treated with concomitant radiation plus temozolomide followed by adjuvant temozolomide. J Clin Oncol. 2002;20:1375–82. http://dx.doi.org/10.1200/JCO.2002.20.5.1375
13. Anton K, Baehring JM, Mayer T. Glioblastoma multiforme: Overview of current treatment and future perspectives. Hematol Oncol Clin North Am. 2012;26(4):825–53. http://dx.doi.org/10.1016/j.hoc.2012.04.006
14. Siu A, Wind JJ, Iorgulescu JB, Chan TA, Yamada Y, Sherman JH. Radiation necrosis following treatment of high grade glioma-a review of the literature and current understanding. Acta Neurochir. 2012;154(2):191–201. http://dx.doi.org/10.1007/s00701-011-1228-6
15. van den Bent MJ. Practice changing mature results of RTOG study 9802: Another positive PCV trial makes adjuvant chemotherapy part of standard of care in low-grade glioma. Neuro Oncol. 2014;16(12):1570–4. http://dx.doi.org/10.1093/neuonc/nou297
16. de Vries NA, Beijnen JH, van Tellingen O. High-grade glioma mouse models and their applicability for preclinical testing. Cancer Treat Rev. 2009;35:714–23. http://dx.doi.org/10.1016/j.ctrv.2009.08.011
17. Gorlia T, van den Bent MJ, Hegi ME, Mirimanoff RO, Weller M, Cairncross JG, et al. Nomograms for predicting survival of patients with newly diagnosed glioblastoma: Prognostic factor analysis of EORTC and NCIC trial 26981-22981/CE.3. Lancet Oncol. 2008;9:29–38. http://dx.doi.org/10.1016/S1470-2045(07)70384-4
18. Ducray F, Idbaih A, Wang XW, Cheneau C, Labussiere M, Sanson M. Predictive and prognostic factors for gliomas. Expert Rev Anticancer Ther. 2011;11:781–9. http://dx.doi.org/10.1586/era.10.202
19. Wen PY, Macdonald DR, Reardon DA, Cloughesy TF, Sorensen AG, Galanis E, et al. Updated response assessment criteria for high-grade gliomas: Response assessment in neuro-oncology working group. J Clin Oncol. 2010;28:1963–72. http://dx.doi.org/10.1200/JCO.2009.26.3541

20. Jain R, Narang J, Sundgren PM, Hearshen D, Saksena S, Rock JP, et al. Treatment induced necrosis versus recurrent/progressing brain tumor: Going beyond the boundaries of conventional morphologic imaging. J Neurooncol. 2010;100(1):17–29. http://dx.doi.org/10.1007/s11060-010-0139-3
21. Chao ST, Suh JH, Raja S, Lee SY, Barnett G. The sensitivity and specificity of FDG PET in distinguishing recurrent brain tumor from radionecrosis in patients treated with stereotactic radiosurgery. Int J Cancer. 2001;96:191–7. http://dx.doi.org/10.1002/ijc.1016
22. Lutz K, Radbruch A, Wiestler B, Bäumer P, Wick W, Bendszus M. Neuroradiological response criteria for high-grade gliomas. Clin Neuroradiol. 2011;21:199–205. http://dx.doi.org/10.1007/s00062-011-0080-7
23. Langleben DD, Segall GM. PET in differentiation of recurrent brain tumor from radiation injury. J Nucl Med. 2000;41:1861–7.
24. Ruben JD, Dally M, Bailey M, Smith R, McLean CA, Fedele P. Cerebral radiation necrosis: Incidence, outcomes, and risk factors with emphasis on radiation parameters and chemotherapy. Int J Radiat Oncol Biol Phys. 2006;65(2):499–508. http://dx.doi.org/10.1016/j.ijrobp.2005.12.002
25. Lizarraga KJ, Allen-Auerbach M, Czernin J, DeSalles AA, Yong WH, Phelps ME, et al. 18F-FDOPA PET for differentiating recurrent or progressive brain metastatic tumors from late or delayed radiation injury after radiation treatment. J Nucl Med. 2014;55(1):30–6. http://dx.doi.org/10.2967/jnumed.113.121418
26. Rahmathulla G, Marko NF, Weil RJ. Cerebral radiation necrosis: A review of the pathobiology, diagnosis and management considerations. J Clin Neurosci. 2013;20(4):485–502. http://dx.doi.org/10.1016/j.jocn.2012.09.011
27. Giglio P, Gilbert HR. Cerebral radiation necrosis. Neurologist. 2003;9:180–8. http://dx.doi.org/10.1097/01.nrl.0000080951.78533.c4
28. Van Laere K, Ceyssens S, Van Calenbergh F, de Groot T, Menten J, Flamen P, et al. Direct comparison of 18F-FDG and 11C-methionine PET in suspected recurrence of glioma: Sensitivity, inter-observer variability and prognostic value. Eur J Nucl Med Mol Imaging. 2005;32:39–51. http://dx.doi.org/10.1007/s00259-004-1564-3
29. Hoekstra CJ, Paglianiti I, Hoekstra OS, Smit EF, Postmus PE, Teule GJ, et al. Monitoring response to therapy in cancer using (18F)-2-fluoro-2-deoxy-D-glucose and positron emission tomography—An overview of different analytical methods. Eur J Nucl Med. 2000;27:731–43. http://dx.doi.org/10.1007/s002590050570
30. Dhermain FG, Hau P, Lanfermann H, Jacobs AH, van den Bent MJ. Advanced MRI and PET imaging for assessment of treatment response in patients with gliomas. Lancet Neurol. 2010;9:906–20. http://dx.doi.org/10.1016/S1474-4422(10)70181-2
31. Galldiks N, Langen KJ. Amino acid PET—An imaging option to identify treatment response, posttherapeutic effects, and tumor recurrence? Front Neurol. 2016;28(7):120. http://dx.doi.org/10.3389/fneur.2016.00120
32. Shah A, Snelling B, Bregy A, Patel PR, Tememe D, Bhatia R, et al. Discriminating radiation necrosis from tumor progression in gliomas: A systematic review what is the best imaging modality? J Neurooncol. 2013;112:141–52. http://dx.doi.org/10.1007/s11060-013-1059-9
33. Zeng QS, Li CF, Liu H, Zhen JH, Feng DC. Distinction between recurrent glioma and radiation injury using magnetic resonance spectroscopy in combination with diffusion-weighted imaging. Int J Radiat Oncol Biol Phys. 2007;68:151–8. http://dx.doi.org/10.1016/j.ijrobp.2006.12.001
34. Kim HS, Goh MJ, Kim N, Chol CG, Kim SJ, Kim JH. Which combination of MR imaging modalities is best for predicting recurrent glioblastoma? Study of diagnostic accuracy and reproducibility. Radiology. 2014;273:831–43. http://dx.doi.org/10.1148/radiol.14132868
35. Hu LS, Baxter LC, Smith KA, Feuerstein BG, Karis JP, Eschbacher JM, et al. Relative cerebral blood volume values to differentiate high-grade glioma recurrence from posttreatment radiation effect: Direct correlation between image-guided tissue histopathology and localized dynamic susceptibility-weighted contrast-enhanced perfusion MR imaging measurements. Am J Neuroradiol. 2009;30:552–8. http://dx.doi.org/10.3174/ajnr.A1377
36. Barajas RF Jr, Chang JS, Segal MR, Parsa AT, McDermott MW, Berger MS, et al. Differentiation of recurrent glioblastoma multiforme from radiation necrosis after external beam radiation therapy with

dynamic susceptibility-weighted contrast-enhanced perfusion MR imaging. Radiology. 2009;253: 486–96. http://dx.doi.org/10.1148/radiol.2532090007
37. Zhou J, Tryggestad E, Wen Z, Lal B, Zhou T, Grossman R, et al. Differentiation between glioma and radiation necrosis using molecular resonance imaging of endogeneous proteins and peptides. Nat Med. 2011;17:130–4. http://dx.doi.org/10.1038/nm.2268
38. Parvez K, Parvez A, Zadeh G. The diagnosis and treatment of pseudoprogression, radiation necrosis and brain tumor recurrence. Int J Mol Sci. 2014;15(7):11832–46. http://dx.doi.org/10.3390/ijms150711832
39. Lopci E, Franzese C, Grimaldi M, Zucali PA, Navarria P, Simonelli M, et al. Imaging biomarkers in primary brain tumours. Eur J Nucl Med Mol Imaging. 2015;42(4):597–612. http://dx.doi.org/10.1007/s00259-014-2971-8
40. Demetriades AK1, Almeida AC, Bhangoo RS, Barrington SF. Applications of positron emission tomography in neuro-oncology: A clinical approach. Surgeon. 2014;12(3):148–57. http://dx.doi.org/10.1016/j.surge.2013.12.001
41. Hattingen E, Pilatus U. Brain tumor imaging. Berlin: Springer; 2016. Chapter, PET imaging of brain tumors; p. 121–35. http://dx.doi.org/10.1007/978-3-642-45040-2
42. Frosina G. Positron emission tomography of high-grade gliomas. J Neurooncol. 2016;127:415–25. http://dx.doi.org/10.1007/s11060-016-2077-1
43. Kuge Y, Shiga T, Tamaki N. Perspectives on nuclear medicine for molecular diagnosis and integrated therapy. Japan: Springer; 2016. Chapter 18, Hypoxia imaging with 18F-FMISO PET for brain tumors; p. 236. http://dx.doi.org/10.1007/978-4-431-55894-1
44. Zhang H, Liu N, Gao S, Hu X , Zhao W, Tao R, et al. Can an 18F-ALF-NOTA-PRGD2 PET/CT scan predict treatment sensitivity to concurrent chemoradiotherapy in patients with newly diagnosed glioblastoma? J Nucl Med. 2016; 57:524–9. http://dx.doi.org/10.2967/jnumed.115.165514
45. James ML, Gambhir SS. A molecular imaging primer: Modalities, imaging agents, and applications. Physiol Rev. 2012;92(2):897–965. http://dx.doi.org/10.1152/physrev.00049.2010
46. Doyle WK, Budinger TF, Valk PE, Levin VA, Gutin PH. Differentiation of cerebral radiation necrosis from tumor recurrence by (18F)FDG and 82Rb positron emission tomography. J Comput Assist Tomogr. 1987;11(4):563–70. http://dx.doi.org/10.1097/00004728-198707000-00001
47. Kahn D, Follett KA, Bushnell DL, Nathan MA, Piper JG, Madsen M, et al. Diagnosis of recurrent brain tumor: Value of 201T1 SPECT vs 18F-fluorodeoxyglucose PET. Am J Roentgenol. 1994;163:1459–65. http://dx.doi.org/10.2214/ajr.163.6.7992747
48. Ricci PE, Karis JP, Heiserman JE, Fram EK, Bice AN, Drayer BP. Differentiating recurrent tumor from radiation necrosis: Time for re-evaluation of positron emission tomography? Am J Neuroradiol. 1998;19:407–13.
49. Bolcaen J, Descamps B, Deblaere K, Boterberg T, De Vos F, Kalala JP, et al. 18F-fluoromethylcholine (FCho), 18F-fluoroethyltyrosine (FET), and 18F-fluorodeoxyglucose (FDG) for the discrimination between high-grade glioma and radiation necrosis in rats: A PET study. Nucl Med Biol. 2014;42(1): 38–45. http://dx.doi.org/10.1016/j.nucmedbio.2014.07.006
50. Bolcaen J, Lybaert K, Moerman L, Descamps B, Deblaere K, Boterberg T, et al. Kinetic modeling and graphical analysis of 18F-fluoromethylcholine (FCho), 18F-fluoroethyltyrosine (FET) and 18F-fluorodeoxyglucose (FDG) PET for the discrimination between high-grade glioma and radiation necrosis in rats. PLoS One. 2016;11(10):e0164208. http://dx.doi.org/10.1371/journal.pone.0164208
51. Spaeth N, Wyss MT, Weber B, Scheidegger S, Lutz A, Verwey J, et al. Uptake of 18F-fluorocholine, 18F-fluoroethyl-L-tyrosine, and 18F-FDG in acute cerebral radiation injury in the rat: Implications for separation of radiation necrosis from tumor recurrence. J Nucl Med. 2004;45:1931–8.
52. Spaeth N, Wyss MT, Pahnke J, Biollaz G, Lutz A, Goepfert K, et al. Uptake of 18F-fluorocholine, 18F-fluoro-ethyl-L-tyrosine and 18F-fluoro-2-deoxyglucose in F98 gliomas in the rat. Eur J Nucl Med Mol Imaging. 2006;33:673–82. http://dx.doi.org/10.1007/s00259-005-0045-7
53. Caroline I, Rosenthal MA. Imaging modalities in high-grade gliomas: Pseudoprogression, recurrence, or necrosis? J Clin Neurosci. 2012;19(5):633–7. http://dx.doi.org/10.1016/j.jocn.2011.10.003
54. Nihashi T, Dahabreh IJ, Terasawa T. Diagnostic accuracy of PET for recurrent glioma diagnosis: A meta-analysis. Am J Neuroradiol. 2013;34(5):944–50. http://dx.doi.org/10.3174/ajnr.A3324

55. Mertens K, Acou M, Van Hauwe J, De Ruyck I, Van den Broecke C, Kalala JP, et al. Validation of 18F-FDG PET at conventional and delayed intervals for the discrimination of high-grade from low-grade gliomas: A stereotactic PET and MRI study. Clin Nucl Med. 2013;38(7):495–500. http://dx.doi.org/10.1097/RLU.0b013e318292a753
56. Chen W. Clinical applications of PET in brain tumors. J Nucl Med. 2007;48(9):1468–81. http://dx.doi.org/10.2967/jnumed.106.037689
57. Spence AM, Muzi M, Mankoff DA, O'Sullivan SF, Link JM, Lewellen TK, et al. 18F-FDG PET of gliomas at delayed intervals: Improved distinction between tumor and normal gray matter. J Nucl Med. 2004;45(10):1653–9.
58. Horky LL1, Hsiao EM, Weiss SE, Drappatz J, Gerbaudo VH. Dual phase FDG-PET imaging of brain metastases provides superior assessment of recurrence versus post-treatment necrosis. J Neurooncol. 2011;103(1):137–46. http://dx.doi.org/10.1007/s11060-010-0365-8
59. Juweid ME, Hoekstra OS. Positron emission tomography. New York: Springer-Humana press; 2011. Chapter 16, Brain tumors. Methods Mol Biol. 2011;727:291–315. http://dx.doi.org/10.1007/978-1-61779-062-1
60. Piroth MD, Pinkawa M, Holy R, Nussen S, Stoffels G, Coenen HH, et al. Prognostic value of early (18F)fluoroethyltyrosine positron emission tomography after radiochemotherapy in glioblastoma multiforme. Int J Radiat Oncol Biol Phys. 2011;80:176–84. http://dx.doi.org/10.1016/j.ijrobp.2010.01.055
61. Becherer A, Karanikas G, Szabó M, Zettinig G, Asenbaum S, Marosi C, et al. Brain tumour imaging with PET: A comparison between (18F)fluorodopa and (11C)methionine. Eur J Nucl Med Mol Imaging. 2003;30(11):1561–7. http://dx.doi.org/10.1007/s00259-003-1259-1
62. Ikotun OF, Marquez BV, Huang C, Masuko K, Daiji M, Masuko T, et al. Imaging the L-type amino acid transporter-1 (LAT1) with Zr-89 immunoPET. PLoS One. 2013;15;8(10):e77476.
63. Grosu AL, Astner ST, Riedel E, Nieder C, Wiedenmann N, Heinemann F, et al. An interindividual comparison of O-(2-[18F]fluoroethyl)-L-tyrosine (FET)- and L-[methyl-11C]methionine (MET)-PET in patients with brain gliomas and metastases. Int J Radiat Oncol Biol Phys. 2011;81(4):1049–58. http://dx.doi.org/10.1016/j.ijrobp.2010.07.002
64. Langen KJ, Hamacher K, Weckesser M, Floeth F, Stoffels G, Bauer D, et al. O-(2-(18F)fluoroethyl)-L-tyrosine: Uptake mechanisms and clinical applications. Nucl Med Biol. 2006;33(3):287–94. http://dx.doi.org/10.1016/j.nucmedbio.2006.01.002
65. Langen KJ, Tatsch K, Grosu AL, Jacobs AH, Wackesser M, Sabri O. Diagnostics of cerebral gliomas with radiolabeled amino acids. Dtsch Ärztebl Int. 2008;105(4):55–61.
66. Herholz K, Langen KJ, Schiepers C, Mountz JM. Brain tumors. Semin Nucl Med. 2012;42:356–70. http://dx.doi.org/10.1053/j.semnuclmed.2012.06.001
67. Walter F, Cloughesy T, Walter MA, Lai A, Nghiemphu P, Wagle N, et al. Impact of 3,4-dihydroxy-6-18F-fluoro-L-phenylalanine PET/CT on managing patients with brain tumors: The referring physician's perspective. J Nucl Med. 2012;53(3):393–8. http://dx.doi.org/10.2967/jnumed.111.095711
68. Floeth FW, Sabel M, Stoffels G, Pauleit D, Hamacher K, Steiger HJ, et al. Prognostic value of 18F-fluoroethyl-L-tyrosine PET and MRI in small nonspecific incidental brain lesions. J Nucl Med. 2008;49:730–7. http://dx.doi.org/10.2967/jnumed.107.050005
69. Lapa C, Linsenmann T, Monoranu CM, Samnick S, Buck AK, Bluemel C, et al. Comparison of the amino acid tracers 18F-FET and 18F-DOPA in high-grade glioma patients. J Nucl Med. 2014;55:1611–6. http://dx.doi.org/10.2967/jnumed.114.140608
70. Galldiks N, Langen KJ, Holy R, Pinkawa M, Stoffels G, Nolte KW, et al. Assessment of treatment response in patients with glioblastoma using O-(2-18F-fluoroethyl)-L-tyrosine PET in comparison to MRI. J Nucl Med. 2012;53:1048–57. http://dx.doi.org/10.2967/jnumed.111.098590
71. Galldiks N, Kracht LW, Burghaus L, Thomas A, Jacobs AH, Heiss WD, et al. Use of 11C-methionine PET to monitor the effects of temozolomide chemotherapy in malignant gliomas. Eur J Nucl Med Mol Imaging. 2006;33(5):516–24. http://dx.doi.org/10.1007/s00259-005-0002-5
72. Pöpperl G, Goldbrunner R, Gildehaus FJ, Kreth FW, Tanner P, Holtmannspötter M, et al. O-(2-[18F]fluoroethyl)-L-tyrosine PET for monitoring the effects of convection-enhanced delivery of paclitaxel in patients with recurrent glioblastoma. Eur J Nucl Med Mol Imaging. 2005;32(9):1018–25. http://dx.doi.org/10.1007/s00259-005-1819-7

73. Pöpperl G, Götz C, Rachinger W, Schnell O, Gildehaus FJ, Tonn KC, et al. Serial 0-(2-(18F) fluoroethyl)-L-tyrosine PET for monitoring the effects of intracavitary radioimmunotherapy in patients with malignant glioma. Eur J Nucl Med Mol Imaging. 2006;33:792–800. http://dx.doi.org/10.1007/s00259-005-0053-7
74. Galldiks N, Rapp M, Stoffels G, Fink GR, Shah NJ, Coenen HH, et al. Response assessment of bevacizumab in patients with recurrent malignant glioma using [18F]Fluoroethyl-L-tyrosine PET in comparison to MRI. Eur J Nucl Med Mol Imaging. 2013;40:22–33. http://dx.doi.org/10.1007/s00259-012-2251-4
75. Harris RJ, Cloughesy TF, Pope WB, Nghiemphu PL, Lai A, Zaw T, et al. 18F-FDOPA and 18F-FLT positron emission tomography parametric response maps predict response in recurrent malignant gliomas treated with bevacizumab. Neuro Oncol. 2012;14(8):1079–89. http://dx.doi.org/10.1093/neuonc/nos141
76. Schwarzenberg J, Czernin J, Cloughesy TF, Ellingson BM, Pope WB, Grogan T, et al. Treatment response evaluation using 18F-FDOPA PET in patients with recurrent malignant glioma on bevacizumab therapy. Clin Cancer Res. 2014;20(13):3550–9. http://dx.doi.org/10.1158/1078-0432.CCR-13-1440
77. Hutterer M, Nowosielski M, Putzer D, Waitz D, Tinkhauser G, Kostron H, et al. O-(2-18F-fluoroethyl)-L-tyrosine PET predicts failure of antiangiogenic treatment in patients with recurrent high-grade glioma. J Nucl Med. 2011;52:856–64. http://dx.doi.org/10.2967/jnumed.110.086645
78. Rachinger W, Goetz C, Pöpperl G, Gildehaus FJ, Kreth FW, Holtmannspötter M, et al. Positron emission tomography with O-(2-(18F) fluoroethyl)-l-tyrosine versus magnetic resonance imaging in the diagnosis of recurrent gliomas. Neurosurgery. 2005;57(3):505–11. http://dx.doi.org/10.1227/01.NEU.0000171642.49553.B0
79. Suchorska B, Jansen NL, Linn J, Kretzschmar H, Janssen H, Eigenbrod S, et al. Biological tumor volume in 18FET-PET before radiochemotherapy correlates with survival in GBM. Neurology. 2015;84(7):710–9. http://dx.doi.org/10.1212/WNL.0000000000001262
80. Roelcke U, Bruehlmeier M, Hefti M, Hundsberger T, Nitzsche EU. F-18 choline PET does not detect increased metabolism in F-18 fluoroethyltyrosine-negative low-grade gliomas. Clin Nucl Med. 2012;37:e1–3. http://dx.doi.org/10.1097/RLU.0b013e3182336100
81. Salber D, Stoffels G, Pauleit D, Reifenberger G, Sabel M, Shah NJ, et al. Differential uptake of (18F) FET and (3H)l-methionine in focal cortical ischemia. Nucl Med Biol. 2006;33(8):1029–35. http://dx.doi.org/10.1016/j.nucmedbio.2006.09.004
82. Salber D, Stoffels G, Pauleit D, Oros-Peusquens AM, Shah NJ, Klauth P, et al. Differential uptake of O-(2-18F-fluoroethyl)-L-tyrosine, L-3H-methionine, and 3H-deoxyglucose in brain abscesses. J Nucl Med. 2007;48(12):2056–62. http://dx.doi.org/10.2967/jnumed.107.046615
83. Takenaka S1, Asano Y, Shinoda J, Nomura Y, Yonezawa S, Miwa K, et al. Comparison of (11)C-methionine, (11)C-choline, and (18)F-fluorodeoxyglucose-PET for distinguishing glioma recurrence from radiation necrosis. Neurol Med Chir. 2014;54(4):280–9. http://dx.doi.org/10.2176/nmc.oa2013-0117
84. Herrmann K, Czernin J, Cloughesy T, Lai A, Pomykala KL, Benz MR, et al. Comparison of visual and semiquantitative analysis of 18F-FDOPA-PET/CT for recurrence detection in glioblastoma patients. Neuro Oncol. 2014;16(4):603–9. http://dx.doi.org/10.1093/neuonc/not166
85. Calabria FF, Barbarisi M, Gangemi V, Grillea G, Cascini GL. Molecular imaging of brain tumors with radiolabeled choline PET. Neurosurg Rev. 2016;1–10. http://dx.doi.org/10.1007/s10143-016-0756-1
86. Mertens K, Slaets D, Lambert B, Acou M, De Vos F, Goethals I. PET with (18)F-labelled choline-based tracers for tumour imaging: A review of the literature. Eur J Nucl Med Mol Imaging. 2010;37(11):2188–93. http://dx.doi.org/10.1007/s00259-010-1496-z
87. Kwee SA, Ko JP, Jiang CS, Watters MR, Coel MN. Solitary brain lesions enhancing at MR imaging: Evaluation with fluorine 18-fluorocholine PET. Radiology. 2007;244:557–65. http://dx.doi.org/10.1148/radiol.2442060898
88. Vallabhajosula S. ^{18}F-labelled positron emission tomographic radiopharmaceuticals in oncology: An overview of radiochemistry and mechanisms of tumor localization. Sem Nucl Med. 2007;37:400–19. http://dx.doi.org/10.1053/j.semnuclmed.2007.08.004

89. Nakagami K, Uchida T, Ohwada S, Koibuchi Y, Suda Y, Sekine T, et al. Increased choline kinase activity and elevated phosphocholine levels in human colon cancer. Jpn J Cancer Res. 1999;90(4):419–24. http://dx.doi.org/10.1111/j.1349-7006.1999.tb00764.x
90. DeGrado TR, Coleman RE, Wang S, Baldwin SW, Orr MD, Robertson CN, et al. Synthesis and evaluation of 18F-labeled choline as an oncologic tracer for positron emission tomography: Initial findings in prostate cancer. Cancer Res. 2001;61:110–17.
91. Treglia G1, Giovannini E, Di Franco D, Calcagni ML, Rufini V, Picchio M, et al. The role of positron emission tomography using carbon-11 and fluorine-18 choline in tumors other than prostate cancer: A systematic review. Ann Nucl Med. 2012;26(6):451–61. http://dx.doi.org/10.1007/s12149-012-0602-7
92. Hara T, Kosaka N, Kishi H. Development of (18)F-fluoroethylcholine for cancer imaging with PET: Synthesis, biochemistry, and prostate cancer imaging. J Nucl Med. 2002;43:187–99.
93. Bansal A, Shuyan W, Hara T, Harris RA, Degrado TR. Biodisposition and metabolism of (18F)fluorocholine in 9L glioma cells and 9L glioma-bearing fisher rats. Eur J Nucl Med Mol Imaging. 2008;35:1192–203. http://dx.doi.org/10.1007/s00259-008-0736-y
94. Li W, Ma L, Wang X, Sun J, Wang S, Hu X. 11C-choline PET/CT tumor recurrence detection and survival prediction in post-treatment patients with high-grade gliomas. Tumor Biol. 2014;35:12353–60.
95. Parashar B, Wernicke AG, Rice S, Osborne J, Singh P. Early assessment of radiation response using a novel functional imaging modality-[18F] Fluorocholine PET (FCH-PET): A pilot study. Discov Med. 2012;14:13–20. http://dx.doi.org/10.1007/s13277-014-2549-x
96. Bolcaen J, Acou M, Boterberg T, Vanhove C, De Vos F, Van den Broecke C, et al. ^{18}F-fluoromethylcholine (^{18}F-FCho) PET and MRI for the prediction of response in glioblastoma patients according to the RANO criteria. Nucl Med Commun. 2017;38(3):242–9.
97. Tan H, Chen L, Guan Y, Lin X. Comparison of MRI, F-18 FDG, and 11C-choline PET/CT for their potentials in differentiating brain tumor recurrence from brain tumor necrosis following radiotherapy. Clin Nucl Med. 2011;36:978–81. http://dx.doi.org/10.1097/RLU.0b013e31822f68a6
98. Takesh M. Kinetic modeling application to 18F-fluoroethylcholine positron emission tomography in patients with primary and recurrent prostate cancer using two-tissue compartmental model. World J Nucl Med. 2013;12(3):101–10. http://dx.doi.org/10.4103/1450-1147.136734
99. Challapali A, Sharma R, Hallett WA, Koziowski K, Carroll L, Brickute D, et al. Biodistribution and radiation dosimetry of deuterium-substituted 18F-fluoromethyl-(1,2-$^{2}H_4$)choline in healthy volunteers. J Nucl Med. 2014;55(2):256–63. http://dx.doi.org/10.2967/jnumed.113.129577
100. Roivainen A, Forsback S, Grönroos T, Lehikoinen P, Kähkönen M, Sutinen E, et al. Blood metabolism of (methyl-11C)choline; implications for in vivo imaging with positron emission tomography. Eur J Nucl Med. 2000;27(1):25–32. http://dx.doi.org/10.1007/PL00006658
101. Verwer EE, Oprea-Lager DE, van den Eertwegh AJM, van Moorselaar RJ, Windhorst AD, Schwarte LA, et al. Quantification of 18F-fluorocholine kinetics in patients with prostate cancer. J Nucl Med. 2015;56:365–71. http://dx.doi.org/10.2967/jnumed.114.148007
102. Nordsmark M, Overgaard J. Tumor hypoxia is independent of hemoglobin and prognostic for loco-regional tumor control after primary radiotherapy in advanced head and neck cancer. Acta Oncol. 2004;43(4):396–403. http://dx.doi.org/10.1080/02841860410026189
103. Rajendran JG, Krohn KA. F-18 fluoromisonidazole for imaging tumor hypoxia: Imaging the microenvironment for personalized cancer therapy. Sem Nucl Med. 2015;45(2):151–62. http://dx.doi.org/10.1053/j.semnuclmed.2014.10.006
104. Galldiks N, Langen KJ. Amino acid PET in neuro-oncology: Applications in the clinic. Expert Rev Anticancer Ther. 2017;11:1–3. http://dx.doi.org/10.1080/14737140.2017.1302799
105. Postema EJ, McEwan AJ, Riauka TA, Kumar P, Richmond DA, Abrams DN, et al. Initial results of hypoxia imaging using 1-alpha-D:-(5-deoxy-5-(18F)-fluoroarabinofuranosyl)-2-nitroimidazole (18F-FAZA). Eur J Nucl Med Mol Imaging. 2009;36(10):1565–73. http://dx.doi.org/10.1007/s00259-009-1154-5
106. Mankoff DA, Shields AF, Krohn KA. PET imaging of cellular proliferation. Radiol Clin North Am. 2005;43(1):153–67. http://dx.doi.org/10.1016/j.rcl.2004.09.005

107. Buck AK, Herrmann K, Shen C, Dechow T, Schwaiger M, Wester HJ. Molecular imaging of proliferation in vivo: Positron emission tomography with (18F)fluorothymidine. Methods. 2009;48:205–15. http://dx.doi.org/10.1016/j.ymeth.2009.03.009
108. Barwick T, Bencherif B, Mountz JM, Avril N. Molecular PET and PET/CT imaging of tumour cell proliferation using F-18 fluoro-Lthymidine: A comprehensive evaluation. Nucl Med Commun. 2009;30:908–17. http://dx.doi.org/10.1097/MNM.0b013e32832ee93b
109. Bradbury MS, Hambardzumyan D, Zanzonico PB, Schwartz J, Cai S, Burnazi EM, et al. Dynamic small-animal PET imaging of tumor proliferation with 3'-deoxy-3'-18F-fluorothymidine in a genetically engineered mouse model of high-grade gliomas. J Nucl Med. 2008;49(3):422–9. http://dx.doi.org/10.2967/jnumed.107.047092
110. Jacobs AH, Thomas A, Kracht LW, Li H, Dittmar C, Garlip G, et al. 18F-fluoro-L-thymidine and 11C-methylmethionine as markers of increased transport and proliferation in brain tumors. J Nucl Med. 2005;46(12):1948–58.
111. Price SJ, Fryer TD, Cleij MC, Dean AF, Joseph J, Salvador R, et al. Imaging regional variation of cellular proliferation in gliomas using 3'-deoxy-3'-(18F)fluorothymidine positron-emission tomography: An image-guided biopsy study. Clin Radiol. 2009;64(1):52–63. http://dx.doi.org/10.1016/j.crad.2008.01.016
112. Idema AJ, Hoffmann AL, Boogaarts HD, Troost EG, Wesseling P, Heerschap A, et al. 3'-Deoxy-3'-18F-fluorothymidine PET-derived proliferative volume predicts overall survival in high-grade glioma patients. J Nucl Med. 2012;53:1904–10. http://dx.doi.org/10.2967/jnumed.112.105544
113. Bao X, Wang MW, Zhang YP, Zhang YJ. Early monitoring antiangiogenesis treatment response of Sunitinib in U87MG Tumor Xenograft by (18)F-FLT MicroPET/CT imaging. Biomed Res Int. 2014;2014:218578. http://dx.doi.org/10.1155/2014/218578
114. Corroyer-Dulmont A, Pérès EA, Gérault AN, Savina A, Bouquet F, Divoux D. Multimodal imaging based on MRI and PET reveals ((18)F)FLT PET as a specific and early indicator of treatment efficacy in a preclinical model of recurrent glioblastoma. Eur J Nucl Med Mol Imaging. 2016;43(4):682–94. http://dx.doi.org/10.1007/s00259-015-3225-0
115. Viel T, Schelhaas S, Wagner S, Wachsmuth L, Schwegmann K, Kuhlmann M, et al. Early assessment of the efficacy of temozolomide chemotherapy in experimental glioblastoma using (18F)FLT-PET imaging. PLoS One. 2013;8(7):e67911. http://dx.doi.org/10.1371/journal.pone.0067911
116. Enslow MS, Zollinger LV, Morton KA, Butterfield RI, Kadrmas DJ, Christian PE, et al. Comparison of 18F-fluorodeoxyglucose and 18F-fluorothymidine PET in differentiating radiation necrosis from recurrent glioma. Clin Nucl Med. 2012;37(9):854–61. http://dx.doi.org/10.1097/RLU.0b013e318262c76a
117. Wardak M, Schiepers C, Cloughesy TF, Dahlbom M, Phelps ME, Huang SC. 18F-FLT and 18F-FDOPA PET kinetics in recurrent brain tumors. Eur J Nucl Med Mol Imaging. 2014;41(6):1199–209. http://dx.doi.org/10.1007/s00259-013-2678-2
118. Kamson DO, Juhasz C, Buth A, Kupsky WJ, Barger GR, Chakraborty PK, et al. Tryptophan PET in pretreatment delineation of newly-diagnosed gliomas: MRI and histopathologic correlates. J NeuroOncol. 2013;112:121–32. http://dx.doi.org/10.1007/s11060-013-1043-4
119. Kondo A, Ishii H, Aoki S, Suzuki M, Nagasawa H, Kubota K, et al. Phase IIa clinical study of (18F) fluciclovine: Efficacy and safety of a new PET tracer for brain tumors. Ann Nucl Med. 2016;30:608–18. http://dx.doi.org/10.1007/s12149-016-1102-y
120. Venneti S, Dunphy MP, Zhang H, Pitter KL, Zanzonico P, Campos C, et al. Glutamine-based PET imaging facilitates enhanced metabolic evaluation of gliomas in vivo. Sci Transl Med. 2015;7(274):274ra17. http://dx.doi.org/10.1126/scitranslmed.aaa1009
121. Alkonyi B, Barger GR, Mittal S, Muzik O, Chugani DC, Bahl G, et al. Accurate differentiation of recurrent gliomas from radiation injury by kinetic analysis of alpha-11C-methyl-L-tryptophan PET. J Nucl Med. 2012;53:1058–64. http://dx.doi.org/10.2967/jnumed.111.097881
122. Kamson DO, Mittal S, Robinette NL, Muzik O, Kupsky WJ, Barger GR, et al. Increased tryptophan uptake on PET has strong independent prognostic value in patients with a previously treated high-grade glioma. Neuro Oncol. 2014;16:1373–83. http://dx.doi.org/10.1093/neuonc/nou042

123. Su Z, Herholz K, Gerhard A, Roncaroli F, Du Plessis D, Jackson A, et al. ((11)C)-(R)PK11195 tracer kinetics in the brain of glioma patients and a comparison of two referencing approaches. Eur J Nucl Med Mol Imaging. 2013;40:1406–19. http://dx.doi.org/10.1007/s00259-013-2447-2
124. Su Z, Roncaroli F, Durrenberger PF, Coope DJ, Karabatsou K, Hinz R, et al. The 18-kDa mitochondrial translocator protein in human gliomas: A 11C-(R)PK11195 PET imaging and neuropathology study. J Nucl Med. 2015;56,512–17. http://dx.doi.org/10.2967/jnumed.114.151621
125. Winkeler A, Boisgard R, Awde A, Dubois A, Thézé B, Zheng J, et al. The translocator protein ligand (18F)DPA-714 images glioma and activated microglia in vivo. Eur J Nucl Med Mol Imaging. 2012;39:811–23. http://dx.doi.org/10.1007/s00259-011-2041-4
126. Awde AR, Boisgard R, Theze B, Dubois A, Zheng J, Dollé F, et al. The translocator protein radioligand 18F-DPA-714 monitors antitumor effect of erufosine in a rat 9L intracranial glioma model. J Nucl Med. 2013;54:2125–31. http://dx.doi.org/10.2967/jnumed.112.118794
127. Oborski MJ, Laymon CM, Qian Y, Liebermann FS, Nelson AD, Mountz JM. Challenges and approaches to quantitative therapy response assessment in glioblastoma multiforme using the novel apoptosis positron emission tomography tracer F-18 ML-10. Transl Oncol. 2014;7(1):111–9. http://dx.doi.org/10.1593/tlo.13868
128. Allen-Auerbach M, Weber WA. Measuring response with FDG-PET: Methodological aspects. The Oncologist. 2009;14:369–77. http://dx.doi.org/10.1634/theoncologist.2008-0119S